Instrumentation Science & Technology
Publication details, including instructions for authors and subscription information:
http://www.tandfonline.com/loi/list20

A NEW, AUTOMATED, MULTIANGULAR RADIOMETER INSTRUMENT FOR TOWER-BASED OBSERVATIONS OF CANOPY REFLECTANCE (AMSPEC II)

Thomas Hilker [a] , Zoran Nesic [b] , Nicholas C. Coops [a] & Dominic Lessard [b]

[a] Faculty of Forest Resources Management, University of British Columbia, Vancouver, British Columbia, Canada

[b] Faculty of Land and Food Systems, University of British Columbia, Vancouver, British Columbia, Canada

Available online: 15 Sep 2010

To cite this article: Thomas Hilker, Zoran Nesic, Nicholas C. Coops & Dominic Lessard (2010): A NEW, AUTOMATED, MULTIANGULAR RADIOMETER INSTRUMENT FOR TOWER-BASED OBSERVATIONS OF CANOPY REFLECTANCE (AMSPEC II), Instrumentation Science & Technology, 38:5, 319-340

To link to this article: http://dx.doi.org/10.1080/10739149.2010.508357

Instrumentation Science and Technology, 38:319–340, 2010

ISSN: 1073-9149 print/1525-6030 online
DOI: 10.1080/10739149.2010.508357

Taylor & Francis
Taylor & Francis Group

A NEW, AUTOMATED, MULTIANGULAR RADIOMETER INSTRUMENT FOR TOWER-BASED OBSERVATIONS OF CANOPY REFLECTANCE (AMSPEC II)

Thomas Hilker,[1] Zoran Nesic,[2] Nicholas C. Coops,[1] and Dominic Lessard[2]
[1]*Faculty of Forest Resources Management, University of British Columbia, Vancouver, British Columbia, Canada*
[2]*Faculty of Land and Food Systems, University of British Columbia, Vancouver, British Columbia, Canada*

□ *Plant photosynthesis is critical for understanding carbon cycling at landscape and global scales. While tower-based measurements of CO_2 have enhanced our knowledge of ecosystem fluxes, scaling these measurements globally is difficult. Satellite observations provide full, global coverage and hold the potential of spatially continuous measurements of ecosystem fluxes, but the requirements for modeling these fluxes from satellite-derived surface parameters are not well understood. This article describes the further development of a tower-mounted, automated, multiangular spectroradiometer system (AMSPEC II) used to study the relationships between canopy-reflectance and plant-physiological processes from multiangular observations, thereby facilitating a comprehensive modeling of the bidirectional reflectance distribution of the canopy. A Webcam permits simultaneous monitoring of phenological changes over time.*

Keywords multi-angular, photosynthesis, physiology, PRI, radiometer, remote sensing

INTRODUCTION

Continuous monitoring of plant physiological processes, such as photosynthesis, is critical for our understanding of ecosystem functioning, including the cycling of water, nutrients, and carbon.[1,2] As a central approach to measuring the exchange of CO_2 between the land surface and the atmosphere, the eddy-covariance (EC) technique has greatly improved our knowledge of energy and carbon budgets over recent years; these observations, however, are spatially discrete,[3,4] and upscaling of measurements over larger areas is difficult. As a result, considerable

Address correspondence to Thomas Hilker, Faculty of Forest Resources Management, University of British Columbia, 2424 Main Mall, Vancouver, BC V6T 1Z4, Canada. E-mail: thomas.hilker@ubc.ca

uncertainties remain in the prediction of carbon, water, and energy balances at landscape and global scales.[5–8]

As a complement to direct measurements of ecosystem exchange, recent advances in high-resolution optical sensors have allowed the scientific community to reassess the potential of determining physiological processes from remote sensing.[9,10] Based on the understanding that plant physiological properties are related to the biochemical composition of foliage, narrow waveband spectral absorption features can be used to quantify physiological properties, typically in a spectral range of about 400–2500 nm wavelengths.[11] For instance, leaf pigments, such as chlorophylls or carotenoids, absorb light at specific narrow ranges of the visible part of the spectrum (400–700 nm) and, as a result, the reflectance measured at these wavebands can be used to predict the abundances of such pigments in a leaf.[12–16]

Optical remote sensing has the potential to provide full, global coverage via satellite observations, thereby promising a spatially continuous assessment of ecosystem fluxes;[17] however retrieval of biochemical processes from space is challenging.[18] First, spectral reflectance is affected by numerous other factors such as the sun-observer geometry, atmospheric scattering, soil background effects, leaf-angle distribution, leaf area and canopy structure, and second, spatial and temporal dynamics of some of these processes require a high spatial and temporal resolution (sensor revisit time) of observations, which is not yet possible with the existing platforms.[19–21]

One possible way to address these issues and to investigate the scaling requirements for modeling ecosystem fluxes from satellite-derived land surface parameters is to study the relationships between canopy reflectance and plant physiological processes at the stand level, thereby building upon existing networks of eddy–flux measurements.[19,22–24] Tower-based, stand-level remote sensing has the advantage that observations are more easily verifiable than those of air or space-borne observations, such as 1) measurements can be made in a temporally continuous mode, and 2) the spatial origin or "footprint" of tower-based remote sensing is similar to that of the eddy-covariance technique.[25,26] As a result, tower-based observations are useful to investigate the relationship between stand-level optical properties and ecosystem processes and may ultimately help to scale these findings to space.[26–28]

Recently, scientific networks, such as Fluxnet[22] or the SpecNet community,[24] have been established to study the relationship between spectral and flux-tower measurements with the ultimate goal of determining ecosystem fluxes in a spatially and temporally continuous mode. A primary challenge, especially in interpreting optical measurements, lies in the diversity of sampling instruments, methods, and scales,[24] and, as a result, there is a need for documentation and standardization to allow for intercomparison

of data and findings across participating scientific research groups and communities.

As a suggestion to the Fluxnet and SpecNet communities, this technical note describes the implementation of an automated multiangular spectroradiometer instrument (Amspec II), which is based on a prototype system (Amspec I[29]) that has been successfully tested for a period of over three years at various research sites throughout British Columbia (Canada). The new instrument has been designed as an open-source, modular system, largely based on commercially available, off-the-shelf components.

BACKGROUND

A particular focus of remote sensing research during recent years has been the determination of gross primary production (GPP), defined as the gross carbon uptake of plants through photosynthesis. GPP can be calculated as the product of the absorbed photosynthetically active radiation (APAR) and the photosynthetic light use efficiency (ε [g C MJ^{-1}]).[30,31] While considerable progress has been made in determining APAR from satellite remote sensing,[32–34] and numerous studies exist to scale these observations to global levels,[35–37] the determination of ε is more challenging. A possible way to remotely sense ε is by observing the state of a group of leaf pigments called xanthophylls, which are responsible for balancing light absorption and utilization in leaves.[38] Gamon et al.[12,13] demonstrated a principle relationship between the xanthophyll cycle and the Photochemical Reflectance Index (PRI), a narrow waveband spectral index defined as,

$$\mathrm{PRI} = \frac{\rho_{531} - \rho_{570}}{\rho_{531} + \rho_{570}} \tag{1}$$

where ρ_{531} and ρ_{570} is the reflectance at 531 and 570 nm, respectively.[12] This relationship is, however, also affected by numerous other factors such as the sun-view geometry, soil background reflectance, species and canopy characteristics, and pigment pool size,[19,39–43] which makes upscaling of findings to the landscape level rather complex.

Using the Amspec prototype, Hilker et al.[19] demonstrated an approach to address this issue from continuous, multiangular PRI observations. These multiangular measurements can be used to describe the anisotropy of the vegetation surface[21,44,45] and to characterize PRI as a function of the sun–observer geometry, the sky condition at the time of measurement, and the physiological status of the vegetation canopy observed (i.e., ε).[19] The physiological signal contained in PRI may be separated from directional impacts and reflectance effects related to sky conditions by stratifying spectra into homogeneous subsets of observations

with respect to both sky conditions and EC measured ε and subsequent modeling of the bidirectional reflectance distribution (BRDF) of each of these strata.[19] Using this technique, Hilker et al.[19] found a strong, nonlinear relationship between ε and stand-level PRI using continuous, year-round spectral observations. The work also demonstrated a strong dependency of ε and PRI on canopy shading and structure, thereby emphasizing the need for multi-angular measurements.[19,40] Additionally, more recent results[46] show evidence that the relationship between PRI and ε also holds at more general scales using satellite data.

IMPROVEMENTS IN AMSPEC II

The improvements implemented in Amspec II are based on the experiences made with the prototype version. One of the most important findings with Amspec I was the usefulness of multiangular observations for scaling of PRI through the modeling the BRDF. Amspec I, however, was restricted to a single vertical zenith angle (VZA) of 63°, which limited our ability to predict reflectance at other angles. Amspec II now features a pan-tilt unit (PTU) to support measurements at numerous vertical and horizontal angles, thereby allowing for more comprehensive modeling of the BRDF and the investigation of foliage clumping effects on PRI.[47] The ability to programmatically define the sensor position vertically and horizontally also allows for additional features including the tracking of solar and satellite movements (see section "Software"). This is especially useful when comparing tower data to space-borne observations, as it avoids the requirement for modeling differences in the sensor geometries.

Another need identified from Amspec I was the ability to determine seasonal changes in vegetation. A high-resolution camera has now been implemented with the system to allow phenological assessments,[48] together with spectral analysis, and potentially an additional assessment of canopy shading from digital photography.

HARDWARE COMPONENTS

System Overview

Figure 1 shows a schematic drawing of Amspec II. The system consists of two modules, one of which is mounted at the top of the tower, while the control unit is placed at the bottom. The tower module features a spectroradiometer (Unispec DC, PP-Systems, Amesbury, MA, USA), a pan-tilt unit (PTU-D46-17.5W, Directed Perception, Burlingame, CA, USA) and, optionally, a high resolution Webcam (NetCam SC 5MP, StarDot, Buena Park,

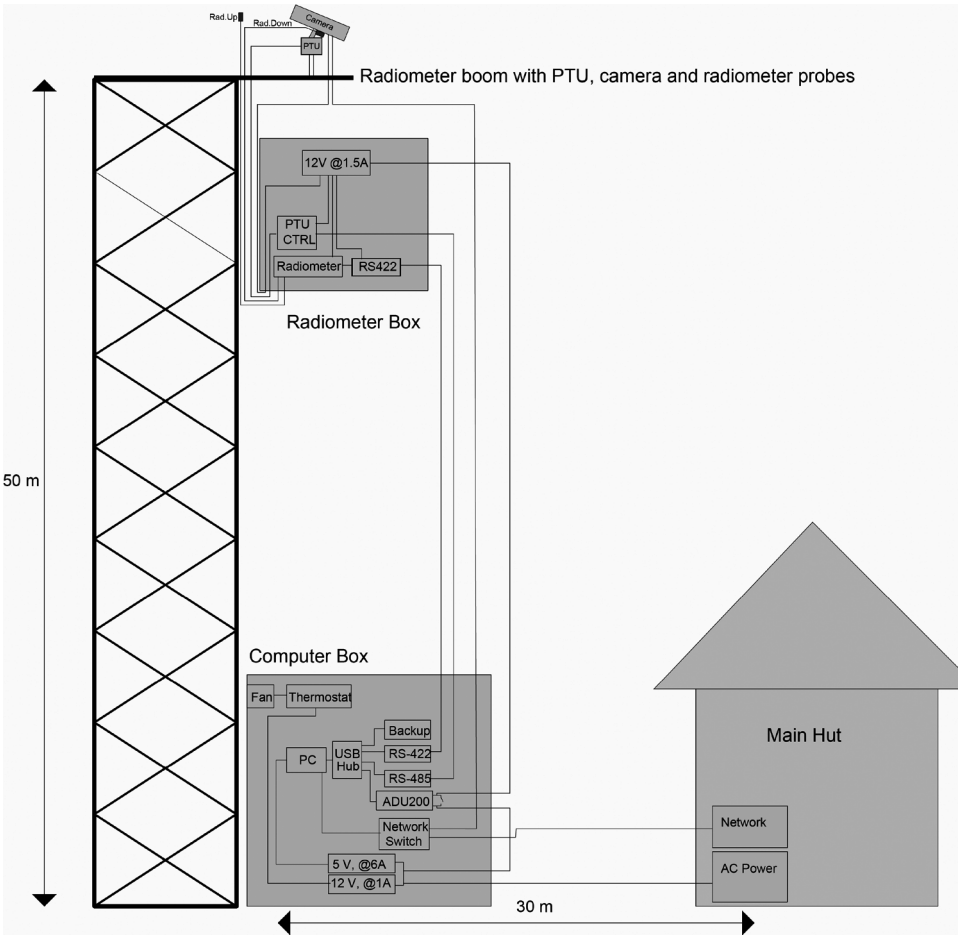

FIGURE 1 Schematic drawing of Amspec II. The system consists of a tower and a control module. The tower module features a spectroradiometer, a pan-tilt unit, and, optionally, a high-resolution Webcam control and tower module are connected via serial communication.

CA, USA). The control module houses a computer and various other devices. Communication between computer and spectroradiometer and between computer and PTU is ensured via serial connections (RS-422/RS-485 standard, respectively, for long-distance communication); the Webcam is connected via a local area network (LAN). The system can be linked to an external network or mobile communication device to allow remote access to the data.

Tower Module

Figure 2 shows a photograph of the tower module, including the spectroradiometer, a control unit for the PTU, and an AC converter for the

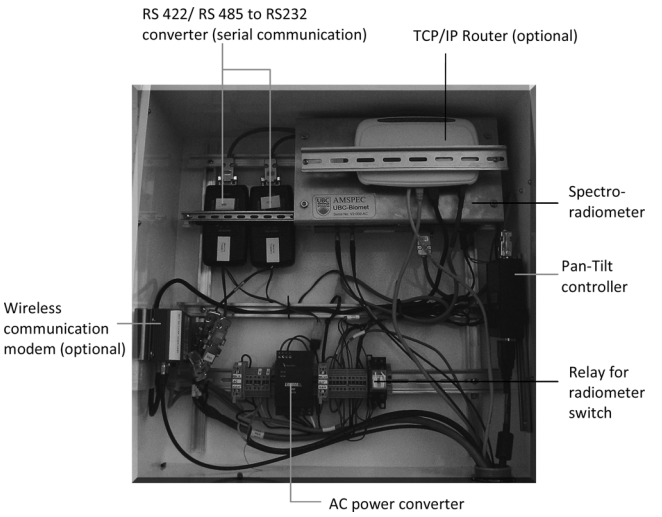

FIGURE 2 Tower module including the spectroradiometer, a control unit for the PTU, an AC converter for the main power supply, and communication devices for serial and Internet communication.

main power supply. The spectroradiometer implemented in Amspec II is a Unispec-DC system featuring 256 contiguous bands with a band spacing of 3 nm [10 nm full width half maximum (FWHM) spectral response] and a nominal range of operation between 350 and 1200 nm. To allow sampling under varying sky conditions, the instrument is equipped with two channels that measure solar irradiance and canopy reflectance simultaneously. Spectral measurements are driven by a microcontroller, which incorporates a curved grating that focuses the dispersed light across a fixed 256-element photodiode array. Each channel is connected to a probe via a 2 m fiber optics cable (PP-Systems); the foreoptics of the downward-looking probe has been extended to 4 m in order to allow a greater range of movement.

The pan-tilt controller is part of the PTU package and controls the motors for pan and tilt of the sensor head (see Figure 3). Both, the spectroradiometer and the PTU require an RS-232 serial communication standard, and as a result, the RS-422/RS-485 long distance serial communication from the computer module is converted back into RS-232 using two RS-422/RS-485 to RS-232 converters (B&B Electronics, Ottawa, IL, USA). The power supply of the tower unit is controlled by the computer module and cycled every night to reset the tower system. As the radiometer implemented in Amspec II contains an internal battery, its power is also switched using an additionally relay to ensure it is restarted every night. Optionally, the system can be equipped with a modem and a router to allow remote access via mobile phone communication (as shown in Figure 2).

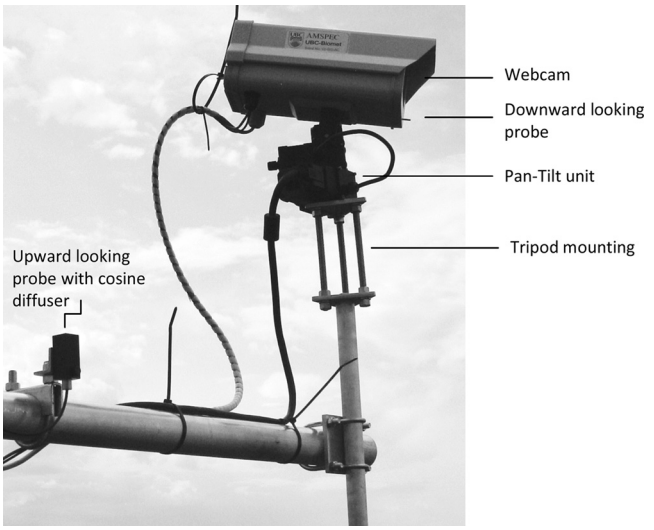

FIGURE 3 Sensor head, including a pan-tilt unit, the upward- and downward-looking radiometer probes, and a Webcam.

Sensor Head

The sensor head, including the Webcam, the upward- and downward-looking radiometer probes, and the PTU, is shown in Figure 3. The upward-pointing probe is equipped with a cosine receptor (PP-Systems) to correct sky irradiance measurements for varying solar altitudes. The downward-looking probe is contained in the camera housing and looks out through a hole in the front. Its instantaneous field of view (IFOV) is about 20°; the footprint of each measurement at canopy height depends on the height of installation above the canopy and the current viewing geometry (horizontal and vertical angles). The sensor head is mounted on a tripod setup sitting on top of the boom in order to allow a better horizontal adjustment of the system.

Computer Module

The computer module features a low power Windows® XP computer (Ultraclient, Norhtec Corporation, Ltd., Thailand), a USB hub (DUB-H7, Dlink, ON, Canada), a USB controllable four-relay interface (ADU200, Ontrak, ON, Canada), AC power converters for 12 V (radiometer, PTU) and 5 V (PC) output, respectively, and a network switch to allow LAN communication (Figure 4). Serial communication to the PTU and the

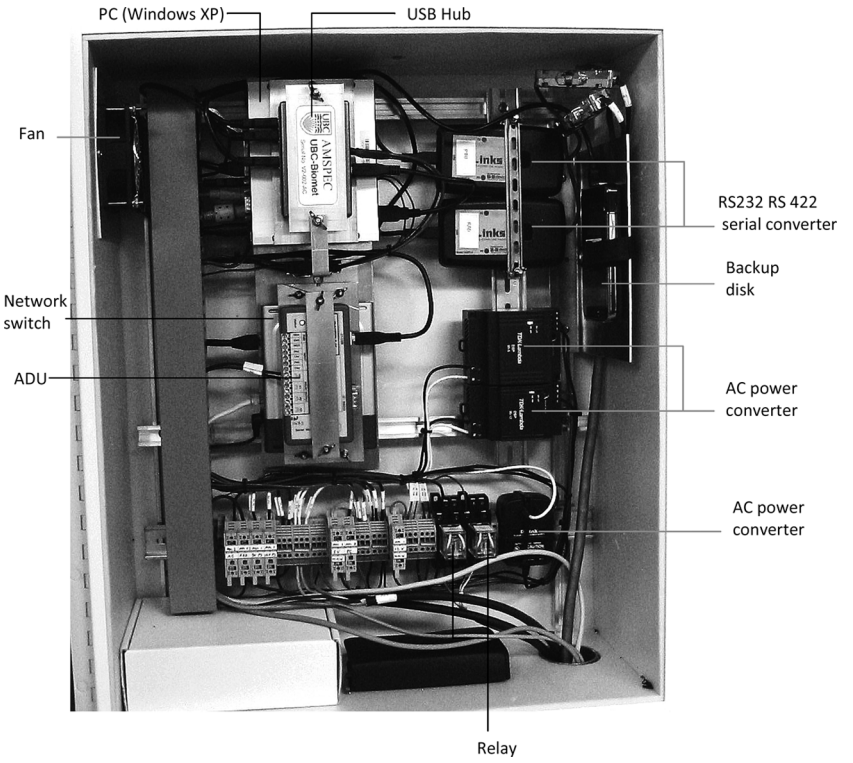

FIGURE 4 Computer module featuring a computer, a USB hub, a USB controllable relay, and AC power converters for 12 V and 5 V output, respectively.

spectroradiometer is ensured by converting the RS-232 communication standard to a long distance RS-422 standard, thereby allowing a cable length of up to 1200 m. If the distance between the computer module and the tower module is less than 50 m, RS-422 converters would not be necessary and RS-232 would suffice. The ADU200 interrupts the power supply of the tower unit every time the computer is being rebooted to ensure an automatic reset of all the peripheral devices. Collected data are backed up automatically every day to an external disk (250 GB), large enough to hold several months of data volume. The system's power is regulated via two external relays to allow a remote and automatic reset. This is useful if power is limited at the site (the system can be shut down overnight when the measurements are not performed to conserve power) or if the computer unit locks up. An external fan prevents the system from overheating when the internal temperature exceeds 40°C. While not discussed here in detail, the wiring diagrams for the tower and computer module are presented in Appendix 1 and 2, respectively.

SOFTWARE

The software controlling Amspec II has been written in Matlab® (Mathworks, Inc., MA, USA), and the source code as well as the compiled version that does not require a Matlab licence are freely available upon request from the authors. The system is designed to work fully automatically using regularly triggered events to move the PTU, acquire images and spectra from the Webcam and radiometer, respectively, and save and backup the data. Several timeout controls monitor the communication between computer and tower unit and reset individual components in case of a communication failure. Data are written to file every 15 minutes using an automatically generated filename of the format YYMMDDQQ, where QQ is the two-digit running number of the respective quarter-hour interval. Amspec II operates in Universal Standard Time (UTC) to ensure compatibility of the measurements with other data acquired at a flux tower site.

The PTU drives to a sequence of user-defined positions, and this is repeated every 15 minutes to allow the acquisition of spectra at user-defined vertical and horizontal angles per quarter hour interval. (Technical limitations require the vertical zenith angle of the PTU to be $35° \geq \theta \leq 90°$.) In addition to the user-defined positions, the system also acquires spectra (and photographs) in the solar plane at the beginning of each 15-minute sequence to observe the hot- and darkspot of the bidirectional reflectance distribution function (BRDF). The solar position is automatically computed from the system time.[49] In order to allow a direct comparison between Amspec II–acquired spectra and satellite-based observation, Amspec II tracks any user-specified, earth-observing, remote-sensing satellite, thereby driving the radiometer probe to mimic the satelite's viewing geometry every time it passes over the site of installation. The satellite tracking algorithm is based on the NORAD two-line element sets (TLEs) together with the associated SGP4/SDP4 orbital model[50,51] for predicting satellite ephemerides. These two-line element sets describe a platform's orbital parameters and are available online for most scientifically used satellites (http://celestrak.com/NORAD/elements/). Amspec II should be updated with the latest version of these TLEs on a regular basis to ensure the accuracy of the satellite tracking performed by the system.

SENSOR OPERATION

Installation

Two Amspec II instruments have been built and installed in May 2009 at flux tower sites of the Canadian Carbon Program—one on Vancouver Island, British Columbia (DF-49, latitude 49.8688° N, longitude 125.3351 ° W),

and one in Northern Saskatchewan (SOA, latitude 53.6289° N, longitude 106.19779° W), Canada. The DF 49 site is a 60-year-old, second-growth, coniferous forest, located at an elevation of about 300 m above sea level.[52] Douglas fir (*Pseudotsuga menziesii var menziesii* (Mirb.) Franco) is the dominant tree species in this area, with secondary species including western red cedar (*Thuja plicata Donn ex D. Don*) (17%) and western hemlock (*Tsuga heterophylla* (Raf.) (Sarg.)) (3%). The radiometer is mounted on a 45 m tall, 0.51 m triangular, open-lattice–type tower at a height of about 9 m above the canopy. SOA is a mature, 83-year-old Aspen forest (*Populus tremuloides* Michx.) located at 600 m above sea level with a dense understory of hazel (*Corylus cornuta* var. *megaphylla* Victorin nd J. Rousseau). Measurements have been undertaken at this site since 1996 as part of the Boreal Ecosystem Study (BOREAS) and continued as a Boreal Ecosystem Research and Monitoring Sites (BERMS) project. The tower is a 28 m tall, 5 m wide double-scaffold tower; the height of installation was 15 m above the canopy.

Sensor Calibration

Reflectance measured by a dual-channel radiometer is defined as the ratio of canopy radiance and solar irradiance after considering the sensor's differences in sensitivity to light due to the individual photodiodes and foreoptics used in the system. Differences in light sensitivity can be corrected through a cross-calibration approach by measuring the reflectance of a standardized reference target:[53]

$$\rho = \frac{\rho_{canopy}}{\rho_{irradiance}} \frac{\rho'_{irradiance}}{\rho'_{control}}$$

where ρ_{canopy} is the measured radiance of the canopy sensor, $\rho_{irradiance}$ is the simultaneously measured irradiance, $\rho'_{control}$ is the measured radiance of the control surface, and $\rho'_{irradiance}$ is irradiance at the time $\rho'_{control}$ was taken.[29,53] While some of the differences in light sensitivity between the up-looking and the down-looking channels will be eliminated when using normalized difference vegetation indices (such as PRI), light sensitivity may also change with the wavelength at which data is acquired, and, as a result, frequent sensor calibration is necessary to ensure a sufficient data quality. A standardized 5-inch × 5-inch spectralon reference panel (PP-Systems) is being used to calibrate the instrument prior to installation and several times during its operation on the tower.

Dark current (dc) is an electrical current that is generated by thermal electrons in the photocathode of optical instruments.[54] The Unispec-DC does not provide an internal shutter mechanism to automatically correct

for dc, and, as a result, the acquired data can only be corrected in a post-processing step using manual measurements taken with both sensors completely covered from light. Using the Amspec prototype, Hilker et al.[29] demonstrated a principal relationship between the sensor's temperature (as measured by the internal thermometer of the Unispec instrument) and the dc measured when blocking off the light from both sensors, thereby allowing an automated correction of this drift in the measured sensor radiance.

Data Processing

Amspec II records solar irradiance and canopy radiance together with the sensor's viewing geometry, solar position, time of measurement, and the Webcam image. The movement of the PTU is user adjustable. Currently, the probe is moved in 10° horizontal steps between ±175°, thereby completing a full rotation every 15 minutes. At each horizontal location, currently four different vertical angles are measured (alternating between a vertical zenith angle [$\theta \in (48°, 58°, 68°, 78°)$ and $\theta \in (43°, 53°, 63°, 73°)$] every 15 minutes); a measurement in the solar plane is completed at the beginning of every 15-minute interval. A complete list of further user-defined parameters required to run the system is given in Table 1.

Figure 5 shows an example of spectra acquired over a 15-minute interval at DF-49 and SOA, respectively. The variability in reflectance is largely due to the differences in the sun–observer geometry as the sensor observes different locations around the flux tower. Numerous approaches exist to modeling these BRDF effects; one of the most common representations is the semi-empirical kernel approach.[55,56] Kernel-based BRDF models represent angular reflectance distribution as linear superposition of a set of basic BRDF shapes based on relative sun position and simple measures of the canopy structure.[56] These models have the advantage that their parameters can be obtained from mathematical inversion of spectral observations, thereby allowing use over a wide range of scales from canopy level to space-borne observations.[56,57] The semi-empirical kernel representation is given by[55]

$$\rho(\theta_v, \theta_s, \Delta\phi) = k_i + k_g K_L\left(\theta_v, \theta_s, \Delta\phi, \frac{h}{b}, \frac{b}{r}\right) + k_v K_R(\theta_v, \theta_s, \Delta\phi) \qquad (2)$$

where k_i, k_g, and k_v are isotropic, geometric, and volumetric scattering parameters, respectively, and K_L and K_R are the geometric and volumetric BRDF kernels, since temperate forests are most commonly represented by the Li-Sparse[58] and Ross–Thick[59] kernels (LSRT). $\frac{h}{b}$ and $\frac{b}{r}$ are site-specific

TABLE 1 List and Meaning of the Most Important User-Defined Settings

Parameter	Use
Serial port PTU	The serial communication (COM) port of PC to which the PTU is connected
Serial port radiometer	The serial communication (COM) port to which the Radiometer is connected
WebCam IP	The IP address of the Webcam
Webcam image height and width (pixels)	Height and width of the Webcam image to be stored with the data
Max and min PTU positions (°)	User defined maximum and minimum for PTU positions in degree. These variables are intended as additional safety measures to prevent the unit from moving into unwanted vertical and horizontal angles.
Radiometer integration time (ms)	The integration time of the radiometer instrument. This should be defined to balance an optimum signal-to-noise ratio with possible saturations of the measured spectra (default 620 msec).
Number of scans to be averaged	Number of observations made by the Unispec-DC to acquire one output dataset. By default, 10 observations are acquired and averaged (internally) for each spectrum output by the system.
Instrument geographical position (°)	The instrument's latitude and longitude in degrees (required for solar and satellite tracking)
Instrument elevation (m)	Height above sea level in meters (required for solar and satellite tracking)
Time zone (±12)	Time zone in which data is acquired (default UTM = 0)
Bearing of instrument mount (°)	Bearing at which the instrument is mounted at the tower (in degrees) (required for solar and satellite tracking)
Satellite names	List of names of satellites to be tracked by the system
Minimum satellite elevations (°)	Minimum satellite elevation (in degrees) required to track a satellite in the sky. Length must correspond to the number of satellites tracked by system
Satellite orbital parameters	NORAD two-line elements of satellites to be tracked. Number of two-line elements must correspond to number of satellites tracked by the system. The two line elements are provided in an extra file (predict.tle)

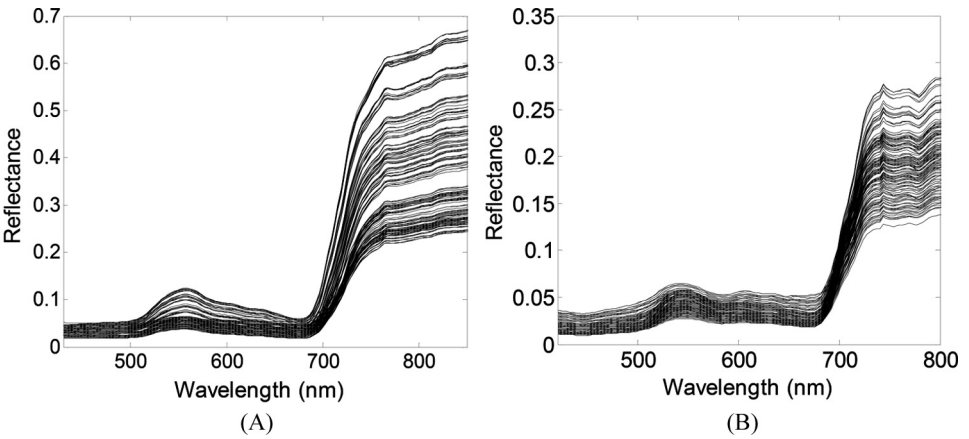

FIGURE 5 Spectra acquired over a 15 minute interval at DF-49 (A) and SOA (B). The variability in reflectance is largely due to the differences in the sun–observer geometry as the sensor observes different locations around the flux tower.

parameters that represent crown relative height crown relative shape.[60] Empirical and semi-empirical BRDF representations are based on the assumption that the physiological status of the observed canopy is constant; this assumption, however, is violated for spectral wavebands that are sensitive to changes in physiological vegetation properties. Hilker et al.[19] demonstrated an approach to modeling BRDF under these heterogonous conditions by stratifying spectra into subsets of observations with respect to the physiological, EC-measured status of the canopy.

Figure 6 shows an example of such a set of BRDF functions modeled for two PRI strata observed at DF-49 (Figure 6A) and SOA (Figure 6B), respectively, at a cloudy and a sunny time interval (15 minutes). On cloudy days, the BRDF functions show only low variability with respect to the view observer geometry, whereas on sunny days there is a clear distinction between sunlit and shaded parts of the canopy. The inversely derived BRDF models can be used to standardize PRI to one common sun–observer geometry using a forward modeling approach with a predefined relative

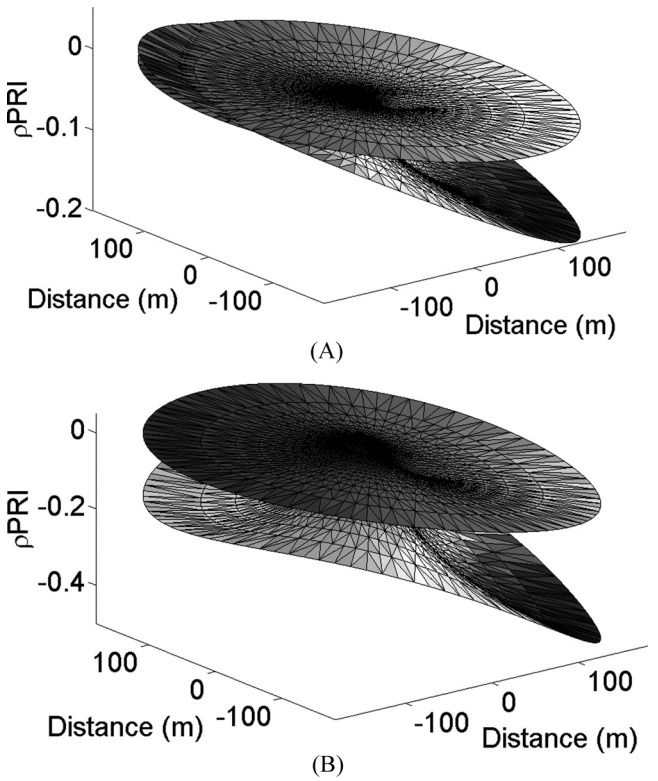

FIGURE 6 BRDF models for two PRI strata observed at DF-49 (A) and SOA (B), at a cloudy and a sunny 15 minute intervals. On cloudy days, the BRDF functions show only low variability with respect to the view observer geometry. On sunny days there is a clear distinction between sunlit and shaded parts of the canopy.

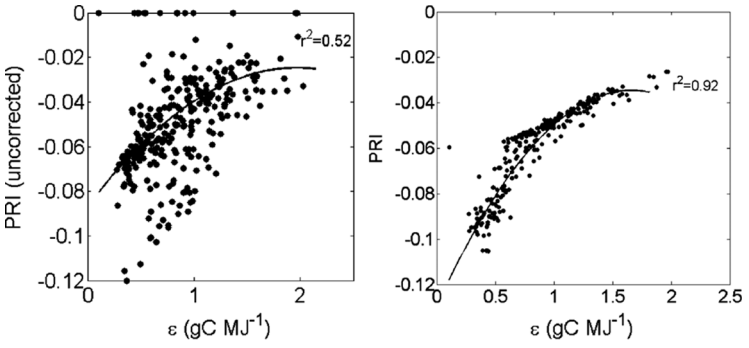

FIGURE 7 Separation of directional and physiological reflectance impacts on daily averaged PRI using year round observations at the DF-49 site. (A) shows a comparison between EC measured ε and PRI measured by the spectrometer directly; (B) shows the result of the stratification approach (figure adapted from Hilker et al.[19]).

sun–sensor position. The differences in the BRDF models shown in either Figure 6A or 6B contain the physiological signal of the PRI observation. The figures also demonstrate the dependency of PRI on canopy shading, as the value of the normalized difference index for the sunlit portion of the canopy is lower (indicating lower ε values) than for the shaded part.[19,40] The result of separating the directional and physiological reflectance impacts on PRI at the DF-49 site using year-round observations (here, based on prototype data) is demonstrated in Figure 7. The method greatly enhanced the relationship between PRI and ε, thereby allowing a year round tracking of stand level ε from spectral observations (see ref.[20] for details).

Figure 8 shows two image composites for DF-49 and SOA, respectively, observed over a 15-minute interval. The photographs have been stitched from 104 (DF-49) and 108 (SOA) individual observations using a normalized cross-correlation approach. The overlap required between two bordering images depends on PTU and Webcam settings and is currently about 25% (angular difference between each observation $= 10°$, size of stored image $= 500 \times 500$ pixels). The areas obscured by the towers (90° at SOA and 100° at DF49) were excluded from the spectral observations and are thus not shown in the figures. The images at SOA were observed under cloudy sky conditions, while the composite shown in Figure 7B has been observed under sunny skies. The difference in reflectance brightness visible in the composites (e.g., Figure 7B) can be used to assess the amount of canopy shading per spectral observation by thresholding image histograms of the RGB channels and defining a simple threshold to classify pixels as either sunlit or shaded.[61]

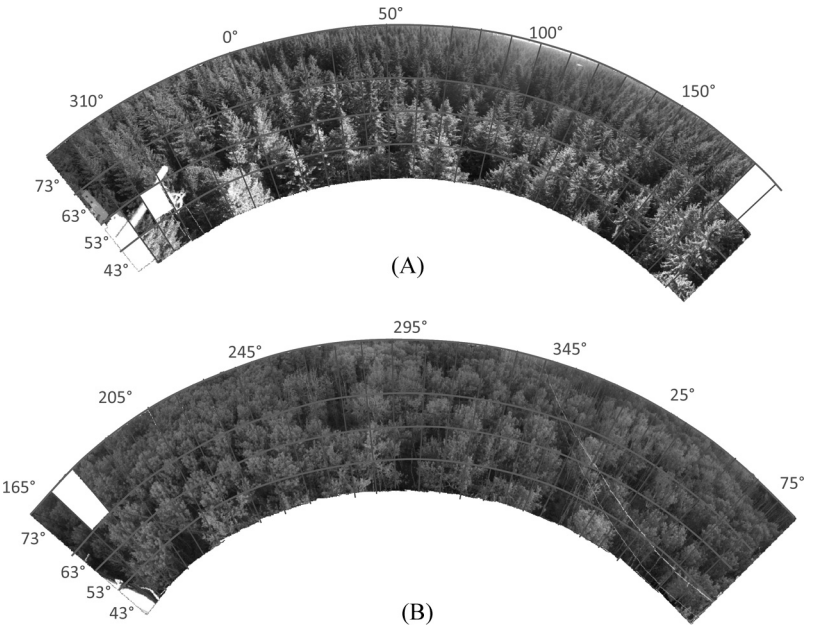

FIGURE 8 Image composites for DF-49 (A) and SOA (B), observed over 15-minute intervals. The photographs have been stitched from 104 (DF-49) and 108 (SOA) individual observations using a normalized cross-correlation approach.

Sensor Costs

Table 2 contains a list of the instruments' components and their approximate costs at the time of purchase. The total sensor costs are a result of the individual components and labor costs (not included in this chart); the majority of the cost is associated with the Unispec DC spectroradiometer.

TABLE 2 Approximate Costs (in U.S. Dollars)

Item	Provider	Date quoted	Qty	Amount
NetCam SC 5 MP Camera, 5 MP	Stardot Tech., 6820 Orangethorpe Ave., Buena Park, CA, 90620, USA	Nov 20, 2008	1	$1,340
PTU-46-17.5 W pan-tilt unit	Directed Perception, 890 C Cowan Road, Burlingame, CA 94010, USA	Nov 21, 2008	1	$2,340
UniSpec-DC dual channel radiometer	PP-Systems, 110 Haverhill Road, Suite 301, Amesbury, MA 01913, USA	Oct 27, 2008	1	$22,750
Computer (Ultra client)	Nor-tech. 901 East Cliff Road, Burnsville, MN 55337, USA		1	$500
Boxes			2	$500
External hard drives			2	$500
Mounts, misc				$500

DISCUSSION AND CONCLUSION

Tower-based eddy-covariance measurements are vital for improving our understanding of vegetation carbon cycling,[1] and they provide valuable inputs to numerous models that simulate fluxes of water and carbon to and from the atmosphere.[62,63] Fundamental differences existing between EC and satellite observations, however, make upscaling of spatially discrete findings to landscape and global levels challenging.[5,7] The instrument described in this article is designed to provide a link between the physiological status of vegetation measurable from CO_2 exchange and the associated changes in spectral reflectance of the plant canopy. For instance, the high spatial, temporal, and spectral detail of observations acquired from Amspec under different view and sun angles allows a comprehensive analysis of spectral reflectance at the stand level. Results using the Amspec prototype[19,26,40,64] have demonstrated a highly significant relationship between canopy reflectance and year-round photosynthesis in a Douglas fir forest, thereby underlying the potential of this method to derive year-round estimates of ε from PRI measurements. Initial findings have also demonstrated that this relationship can be observed from satellite sensors when considering differences in viewing geometry, sensor footprint, and atmospheric effects.[46]

Stand-level analysis is a key for understanding and interpreting satellite observations, which are the result of complex interactions between atmospheric scattering and surface reflectance effects.[46] Based on experiences with the prototype system, we believe that Amspec is a powerful tool for investigating these stand-level relationships and detecting photosynthesis and canopy spectra. Additionally, the innovations introduced with the new version compared to the prototype should help with upscaling tower-based findings more comprehensively by physically matching the sun–observer geometry of different sensor types and observations. A broader validation will, however, be required to generalize this relationship to landscape and global levels. One way to accomplish this is by using a networking approach of several Amspec II–like systems to acquire spectra from multiple flux tower sites simultaneously. A combined effort, including spectral observations of different ecosystems and vegetation types, may significantly improve our understanding of the interactions between stand-level reflectance and plant physiology, and can therefore help with calibrating coarser-scale observations to tower-based measurements.

The importance of plant phenology for detection of vegetation carbon cycling from remote sensing has long been recognized and is documented in numerous studies.[48,65–67] The Webcam system implemented in Amspec II is primarily designed to help address this issue by further investigating the impact of phenological changes on the stand-level photosynthesis and its assessment from spectral reflectance. This is important particularly in broadleaf or grassland ecosystems that show highly distinct seasonal

patterns with likely implications for the prediction of numerous physiological processes at stand- and landscape-level scales.

From an operational point of view, the majority of the sensor cost is associated with the Unispec DC spectroradiometer. While we found this instrument to be very reliable during the operation of the prototype, there are potentially more cost effective alternatives available. For instance, instruments by OceanOptics (Dunedin, FL, USA) have been successfully used in various studies to observe leaf and stand-level chlorophyll and GPP[68,69] and provide a comparable spectral range and resolution. To our knowledge, however, only little experience exists as to how these systems perform when used for continuous monitoring of vegetation properties over longer time periods. For instance, the instrument is more sensitive to differences in temperature and may therefore require a temperature-controlled housing, which increases the costs and energy requirements for the system. Additionally, the use of two-band sensors based on photodiodes-equipped filter glass to allow only certain wavebands to pass may be considered when measurements are required only at specific wavebands (such as 531 and 570 nm for PRI). Further research will be required to investigate these possibilities.

ACKNOWLEDGMENTS

Amspec II has been designed and developed in collaboration with the Biometeorology Group of the faculty of Land and Food Systems. The authors are particularly grateful to Andrew Hum and Rick Ketler for their support in implementing and designing the system. This project has been funded by an NSERC Discovery and NSERC Accelerator grant to Coops. The authors also acknowledge support of the Canadian Caron Program (CCP).

REFERENCES

1. Baldocchi, D. D. Assessing the eddy covariance technique for evaluating carbon dioxide exchange rates of ecosystems: Past, present and future. *Global Change Biol.* **2003**, *9*(4), 479–492.
2. Black, T. A.; Denhartog, G.; Neumann, H. H. Annual cycles of water vapour and carbon dioxide fluxes in and above a boreal aspen forest. *Global Change Biol.* **1996**, *2*(3), 219–229.
3. Reichstein, M.; Papale, D.; Valentini, R.; Aubinet, M.; Bernhofer, C.; Knohl, A.; Laurila, T.; Lindroth, A.; Moors, E.; Pilegaard, K.; Seufert, G. Determinants of terrestrial ecosystem carbon balance inferred from European eddy covariance flux sites. *Geophys. Res. Lett.* **2007**, *34*(1), 1–5.
4. Chen, J.; Ju, W.; Cihlar, J.; Liu, J.; Leblanc, S. G.; Lacaze, R.; Roujean, J. L. Spatial distribution of carbon sources and sinks in Canada's forests. *Tellus Ser. B* **2003**, *55*, 622–641.
5. Heinsch, F. A.; Zhao, M. S.; Running, S. W.; Kimball, J. S.; Nemani, R. R.; Davis, K. J.; Bolstad, P. V.; Cook, B. D.; Desai, A. R.; Ricciuto, D. M.; Law, B. E.; Oechel, W. C.; Kwon, H.; Luo, H. Y.; Wofsy, S. C.; Dunn, A. L.; Munger, J. W.; Baldocchi, D. D.; Xu, L. K.; Hollinger, D. Y.; Richardson, A. D.; Stoy, P. C.; Siqueira, M. B. S.; Monson, R. K.; Burns, S. P.; Flanagan, L. B. Evaluation of remote sensing based terrestrial productivity from Modis using regional tower eddy flux network observations. *IEEE Trans. Geosci. Remote Sens.* **2006**, *44*(7), 1908–1925.

6. Turner, D. P.; Urbanski, S.; Bremer, D.; Wofsy, S. C.; Meyers, T.; Gower, S. T.; Gregory, M. A cross-biome comparison of daily light use efficiency for gross primary production. *Global Change Biol.* **2003**, *9*(3), 383–395.
7. Running, S. W.; Baldocchi, D. D.; Turner, D. P.; Gower, S. T.; Bakwin, P. S.; Hibbard, K. A. A global terrestrial monitoring network integrating tower fluxes, flask sampling, ecosystem modeling and Eos satellite data. *Remote Sens. Environ.* **1999**, *70*(1), 108–127.
8. Hall, F. G.; De Colstoun, E. B.; Collatz, G. J.; Landis, D.; Dirmeyer, P.; Betts, A.; Huffman, G. J.; Bounoua, L.; Meeson, B. Islscp Initiative II global data sets: Surface boundary conditions and atmospheric forcings for land-atmosphere studies. *J. Geophys. Res. Atmos.* **2006**, *111*, D22, 1–2.
9. Curran, P. J. Imaging spectrometry for ecological applications. *Int. J. Appl. Earth Obs. Geoinf.* **2001**, *3*(4), 305–312.
10. Prince, S. D.; Goward, S. N. Global primary production: A remote sensing approach. *J. Biogeogr.* **1995**, *22*(4–5), 815–835.
11. Curran, P. J. Remote-sensing of foliar chemistry. *Remote Sens. Environ.* **1989**, *30*(3), 271–278.
12. Gamon, J. A.; Filella, I.; Penuelas, J., eds. The Dynamic 531-Nanometer Reflectance Signal: A Survey of Twenty Angiosperm Species; *Current Topics in Plant Physiol.* 8, pp. 172–177.
13. Gamon, J. A.; Penuelas, J.; Field, C. B. A narrow-waveband spectral index that tracks diurnal changes in photosynthetic efficiency. *Remote Sens. Environ.* **1992**, *41*(1), 35–44.
14. Datt, B. Remote sensing of chlorophyll a, chlorophyll b, chlorophyll a+b, and total carotenoid content in eucalyptus leaves. *Remote Sens. Environ.* **1998**, *66*(2), 111–121.
15. Zarco-Tejada, P. J.; Miller, J. R.; Mohammed, G. H.; Noland, T. L. Chlorophyll fluorescence effects on vegetation apparent reflectance: I. Leaf-level measurements and model simulation. *Remote Sens. Environ.* **2000**, *74*(3), 582–595.
16. Asner, G. Biophysical and biochemical sources of variability in canopy reflectance. *Remote Sens. Environ.* **1998**, *64*, 234–253.
17. Hall, F. G.; Townshend, J. R.; Engman, E. T. Status of remote-sensing algorithms for estimation of land-surface state parameters. *Remote Sens. Environ.* **1995**, *51*(1), 138–156.
18. Hall, F.; Shimabukuro, Y.; Huemmrich, K. Remote sensing of forest biophysical structure using mixture decomposition and geometric reflectance models. *Ecol. Appl.* **1995**, *5*(4), 993–1013.
19. Hilker, T.; Coops, N. C.; Hall, F. G.; Black, T. A.; Wulder, M. A.; Nesic, Z.; Krishnan, P. Separating physiologically and directionally induced changes in PRI using BRDF models. *Remote Sens. Environ.* **2008**, *112*(6), 2777–2788.
20. Asner, G. P.; Bateson, C. A.; Privette, J. L.; El Saleous, N.; Wessman, C. A. Estimating vegetation structural effects on carbon uptake using satellite data fusion and inverse modeling. *J. Geophys. Res. Atmos.* **1998**, *103*(D22), 28839–28853.
21. Chen, J. M.; Liu, J.; Leblanc, S. G.; Lacaze, R.; Roujean, J. L. Multi-angular optical remote sensing for assessing vegetation structure and carbon absorption. *Remote Sens. Environ.* **2003**, *84*, 516–525.
22. Baldocchi, D.; Falge, E.; Gu, L. H.; Olson, R.; Hollinger, D.; Running, S.; Anthoni, P.; Bernhofer, C.; Davis, K.; Evans, R.; Fuentes, J.; Goldstein, A.; Katul, G.; Law, B.; Lee, X. H.; Malhi, Y.; Meyers, T.; Munger, W.; Oechel, W.; Pilegaard, K. T. P. U. K.; Schmid, H. P.; Valentini, R.; Verma, S.; Vesala, T.; Wilson, K.; Wofsy, S. Fluxnet: A new tool to study the temporal and spatial variability of ecosystem-scale carbon dioxide, water vapor, and energy flux densities. *Bull. Am. Meteorol. Soc.* **2001**, *82*(11), 2415–2434.
23. Margolis, H. A.; Flanagan, L. B.; Amiro, B. D. The Fluxnet-Canada Research Network: Influence of climate and disturbance on carbon cycling in forests and peatlands. *Agric. For. Meteorol.* **2006**, *140*(1–4), 1–5.
24. Gamon, J. A.; Rahman, A. F.; Dungan, J. L.; Schildhauer, M.; Huemmrich, K. F. Spectral Network (Specnet)—What is it and why do we need it? *Remote Sens. Environ.* **2006**, *103*(3), 227–235.
25. Chen, B. Z.; Black, T. A.; Coops, N. C.; Hilker, T.; Trofymow, J. A.; Morgenstern, K. Assessing tower flux footprint climatology and scaling between remotely sensed and eddy covariance measurements. *Boundary-Layer Meteorol.* **2009**, *130*(2), 137–167.
26. Hilker, T.; Coops, N. C.; Hall, F. G.; Black, T. A.; Chen, B.; Krishnan, P.; Wulder, M. A.; Sellers, P. J.; Middleton, E. M.; Huemmrich, K. F. A modeling approach for up-scaling gross ecosystem production to the landscape scale using remote sensing data. *J. Geophys. Res. Biogeosci.* **2008**, *113*, G03006.

27. Leuning, R.; Hughes, D.; Daniel, P.; Coops, N. C.; Newnham, G. A multi-angle spectrometer for automatic measurement of plant canopy reflectance spectra. *Remote Sens. Environ.* **2006**, *103*(3), 236–245.
28. Hilker, T.; Coops, N. C.; Coggins, S.; Wulder, M. A.; Brown, M.; Black, T. A.; Nesic, Z.; Lessard, D. Detection of foliage conditions and disturbance from multi-angular high spectral resolution remote sensing. *Remote Sens. Environ.* **2009**, *113*, 421–434.
29. Hilker, T.; Coops, N. C.; Nesic, Z.; Wulder, M. A.; Black, A. T. Instrumentation and approach for unattended year round tower based measurements of spectral reflectance. *Comput. Electron. Agric.* **2007**, *56*(1), 72–84.
30. Monteith, J. L. Climate and efficiency of crop production in Britain. *Philos. Trans. R. Soc. London, Ser. B* **1977**, *281*(980), 277–294.
31. Monteith, J. L. Solar-radiation and productivity in tropical ecosystems. *J. Appl. Ecol.* **1972**, *9*(3), 747–766.
32. Tucker, C. J.; Sellers, P. J. Satellite remote-sensing of primary production. *Int. J. Remote Sens.* **1986**, *7*(11), 1395–1416.
33. Sellers, P. J. Canopy reflectance, photosynthesis and transpiration. *Int. J. Remote Sens.* **1985**, *6*(8), 1335–1372.
34. Tucker, C. Red and photographic infrared linear combinations for monitoring vegetation. *Remote Sens. Environ.* **1979**, *8*, 127–150.
35. Los, S. O.; Justice, C. O.; Tucker, C. J. A global 1-degrees-by-1-degrees NDVI data set for climate studies derived from the Gimms Continental NDVI data. *Int. J. Remote Sens.* **1994**, *15*(17), 3493–3518.
36. Sellers, P. J.; Tucker, C. J.; Collatz, G. J.; Los, S. O.; Justice, C. O.; Dazlich, D. A.; Randall, D. A. A global 1-degrees-by-1-degrees NDVI data set for climate studies. 2. The generation of global fields of terrestrial biophysical parameters from the NDVI. *Int. J. Remote Sens.* **1994**, *15*(17), 3519–3545.
37. Myneni, R. B.; Hoffman, S.; Knyazikhin, Y.; Privette, J. L.; Glassy, J.; Tian, Y.; Wang, Y.; Song, X.; Zhang, Y.; Smith, G. R.; Lotsch, A.; Friedl, M.; Morisette, J. T.; Votava, P.; Nemani, R. R.; Running, S. W. Global products of vegetation leaf area and fraction absorbed par from year one of Modis data. *Remote Sens. Environ.* **2002**, *83*(1–2), 214–231.
38. Demmig-Adams, B.; Adams, W. W. The role of xanthophyll cycle carotenoids in the protection of photosynthesis. *Trends Plant Sci.* **1996**, *1*(1), 21–26.
39. Barton, C. V. M.; North, P. R. J. Remote sensing of canopy light use efficiency using the photochemical reflectance index—model and sensitivity analysis. *Remote Sens. Environ.* **2001**, *78*(3), 264–273.
40. Hall, F. G.; Hilker, T.; Coops, N. C.; Lyapustin, A.; Huemmrich, F.; Middleton, E.; Margolis, H.; Drolet, G.; Black, T. Multi-angle remote sensing of forest light use efficiency by observing PRI variation with canopy shadow fraction. *Remote Sens. Environ.* **2008**, *112*(7), 3201–3211.
41. Penuelas, J.; Filella, I.; Gamon, J. A. Assessment of photosynthetic radiation-use efficiency with spectral reflectance. *New Phytol.* **1995**, *131*(3), 291–296.
42. Gamon, J. A.; Serrano, L.; Surfus, J. S. The photochemical reflectance index: An optical indicator of photosynthetic radiation use efficiency across species, functional types, and nutrient levels. *Oecologia* **1997**, *112*(4), 492–501.
43. Rahman, A. F.; Gamon, J. A.; Fuentes, D. A.; Roberts, D. A.; Prentiss, D. Modeling spatially distributed ecosystem flux of boreal forest using hyperspectral indices from Aviris imagery. *J. Geophys. Res. Atmos.* **2001**, *106*(D24), 33579–33591.
44. Asner, G. P.; Braswell, B. H.; Schimel, D. S.; Wessman, C. A. Ecological research needs from multiangle remote sensing data. *Remote Sens. Environ.* **1998**, *63*, 155–165.
45. Chen, J.; Leblanc, S. A four-scale bidirectional reflectance model based on canopy architecture. *IEEE Trans. Geosci. Remote Sens.* **1997**, *35*(5), 1316–1337.
46. Hilker, T.; Lyapustin, A.; Hall, F. G.; Wang, Y.; Coops, N. C.; Drolet, G.; Black, T. A. An assessment of photosynthetic light use efficiency from space: Modeling the atmospheric and directional impacts on PRI reflectance. *Remote Sens. Environ.* **2009**, *113*, 2463–2475.
47. Chen, J. M.; Menges, C. H.; Leblanc, S. G. Global mapping of foliage clumping index using multi-angular satellite data. *Remote Sens. Environ.* **2005**, *97*(4), 447–457.
48. Richardson, A. D.; Hollinger, D. Y.; Dail, D. B.; Lee, J. T.; Munger, J. W.; O' Keefe, J. Influence of spring phenology on seasonal and annual carbon balance in two contrasting New England forests. *Tree Physiol.* **2009**, *29*(3), 321–331.
49. Reda, I.; Andreas, A. Solar position algorithm for solar radiation applications. *Sol. Energy* **2004**, *76*(5), 577–589.

50. Crawford, P. S.; Brooks, A. R.; Brush, R. J. H. Fast navigation of AVHRR images using complex orbital models. *Int. J. Remote Sens.* **1996**, *17*(1), 197–212.
51. Kelso, T. S. Validation of SGP4 and IS-GPS-200D against GPS precision ephemerides. Paper presented at the AAS/AIAA 17th Space Flight Mechanics Meeting, Sedona, AZ, USA, Jan. 28–Feb 1, 2007.
52. Morgenstern, K.; Black, T. A.; Humphreys, E. R.; Griffis, T. J.; Drewitt, G. B.; Cai, T. B.; Nesic, Z.; Spittlehouse, D. L.; Livingstone, N. J. Sensitivity and uncertainty of the carbon balance of a Pacific Northwest Douglas-fir forest during an El Nino La Nina Cycle. *Agric. For. Meteorol.* **2004**, *123*(3–4), 201–219.
53. Gamon, J. A.; Cheng, Y. F.; Claudio, H.; MacKinney, L.; Sims, D. A. A mobile tram system for systematic sampling of ecosystem optical properties. *Remote Sens. Environ.* **2006**, *103*(3), 246–254.
54. Bock, R. K. Dark current. Available at: http://rd11.web.cern.ch/RD11/rkb/PH14pp/node40.html, October 2006.
55. Roujean, J. L.; Leroy, M.; Deschamps, P. Y. A bidirectional reflectance model of the earths surface for the correction of remote-sensing data. *J. Geophys. Res. Atmos.* **1992**, *97*(D18), 20455–20468.
56. Wanner, W.; Li, X.; Strahler, A. H. On the derivation of kernels for kernel-driven models of bidirectional reflectance. *J. Geophys. Res. Atmos.* **1995**, *100*(D10), 21077–21089.
57. Wanner, W.; Strahler, A. H.; Hu, B.; Lewis, P.; Muller, J. P.; Li, X.; Schaaf, C. L. B.; Barnsley, M. J. Global retrieval of bidirectional reflectance and albedo over land from Eos Modis and Misr data: Theory and algorithm. *J. Geophys. Res. Atmos.* **1997**, *102*(D14), 17143–17161.
58. Li, X. W.; Strahler, A. H.; Woodcock, C. E. A hybrid geometric optical-radiative transfer approach for modeling albedo and directional reflectance of discontinuous canopies. *IEEE Trans. Geosci. Remote Sens.* **1995**, *33*(2), 466–480.
59. Ross, J. K. *The Radiation Regime and Architecture of Plant Stands*; Dr. W. Junk Publishers: The Hague, 1981.
60. Justice, C.; Markham, B.; Townsend, F.; Kennard, R. Spatial degradation of satellite data. **1989**, *10*(9), 1539–1561.
61. Hilker, T.; Coops, N. C.; Schwalm, C. R.; Jassal, R. S.; Black, T. A.; Krishnan, P. Effects of mutual shading of tree crowns on prediction of photosynthetic light-use efficiency in a coastal Douglas-fir forest. *Tree Physiol.* **2008**, *28*, 825–834.
62. Yuan, W. P.; Liu, S.; Zhou, G. S.; Zhou, G. Y.; Tieszen, L. L.; Baldocchi, D.; Bernhofer, C.; Gholz, H.; Goldstein, A. H.; Goulden, M. L.; Hollinger, D. Y.; Hu, Y.; Law, B. E.; Stoy, P. C.; Vesala, T.; Wofsy, S. C. Deriving a light use efficiency model from eddy covariance flux data for predicting daily gross primary production across biomes. *Agric. For. Meteorol.* **2007**, *143*(3–4), 189–207.
63. Van Dijk, A.; Dolman, A. J. Estimates of CO_2 uptake and release among European forests based on eddy covariance data. *Global Change Biol.* **2004**, *10*(9), 1445–1459.
64. Middleton, E.; Cheng, Y. B.; Hilker, T., et al. Linking foliage spectral responses to canopy-level ecosystem photosynthetic light-use efficiency at a Douglas-fir forest in Canada. *Canadian J. Remote Sens.* **2009**, *35*, 166–188.
65. Nightingale, J. M.; Morisette, J. T.; Wolfe, R. E.; Tan, B.; Gao, F.; Ederer, G.; Collatz, G. J.; Turner, D. P. Temporally smoothed and gap-filled MODIS land products for carbon modelling: Application of the fPAR product. *Int. J. Remote Sens.* **2009**, *30*(4), 1083–1090.
66. Piao, S. L.; Friedlingstein, P.; Ciais, P.; Viovy, N.; Demarty, J. Growing season extension and its impact on terrestrial carbon cycle in the Northern Hemisphere over the past 2 decades. *Global Biogeochem. Cycles* **2007**, *21*(3).
67. Van Wijk, M. T.; Williams, M.; Laundre, J. A.; Shaver, G. R. Interannual variability of plant phenology in tussock tundra: Modelling interactions of plant productivity, plant phenology, snowmelt and soil thaw. *Global Change Biol.* **2003**, *9*(5), 743–758.
68. Schalles, J. F.; Gitelson, A. A.; Yacobi, Y. Z.; Kroenke, A. E. Estimation of chlorophyll a from time series measurements of high spectral resolution reflectance in an eutrophic lake. *J. Phycol.* **1998**, *34*(2), 383–390.
69. Gitelson, A. A.; Vina, A.; Verma, S. B.; Rundquist, D. C.; Arkebauer, T. J.; Keydan, G.; Leavitt, B.; Ciganda, V.; Burba, G. G.; Suyker, A. E. Relationship between gross primary production and chlorophyll content in crops: Implications for the synoptic monitoring of vegetation productivity. *J. Geophys. Res. Atmos.* **2006**, *111*(D8).

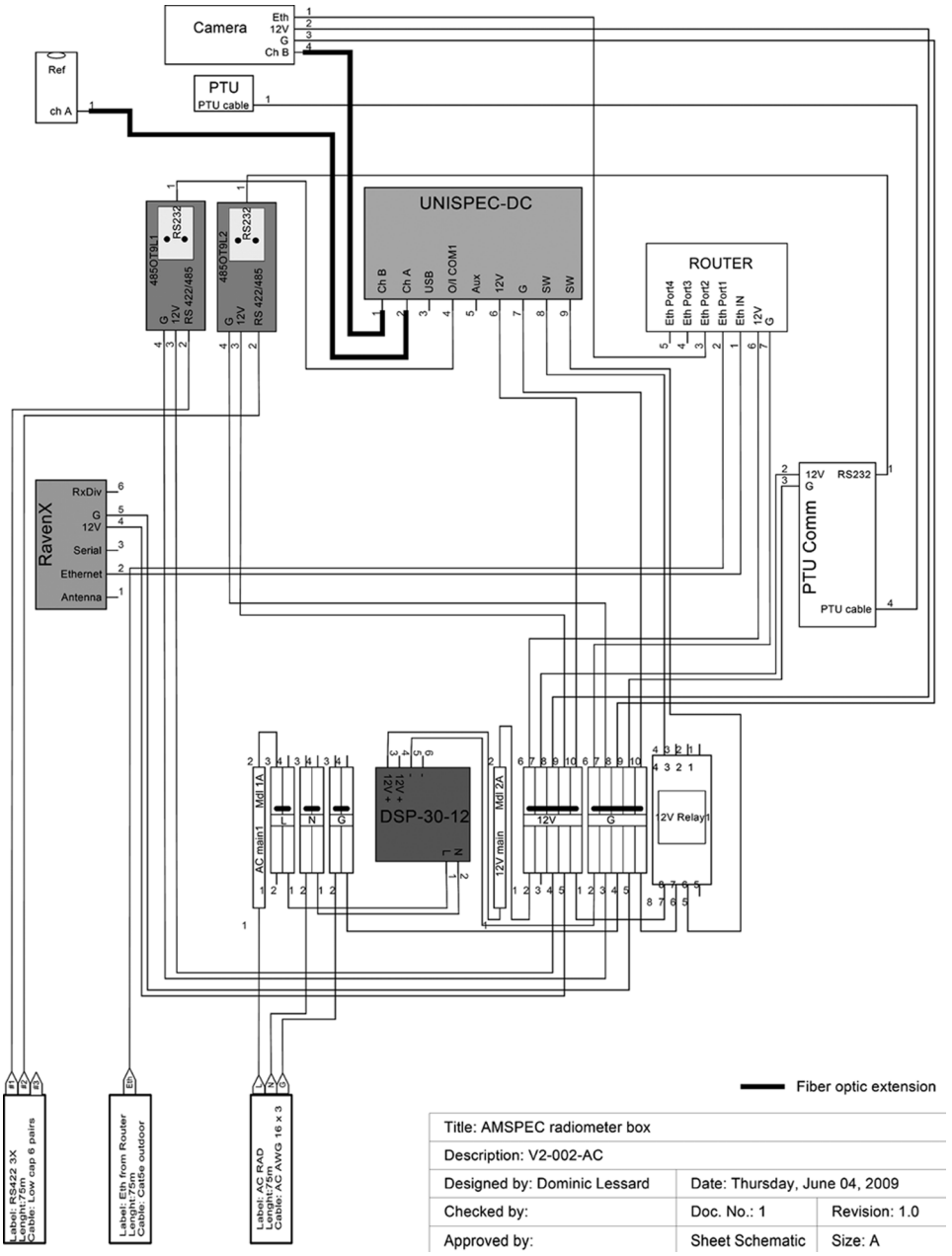

APPENDIX 1 Wiring diagrams tower module.

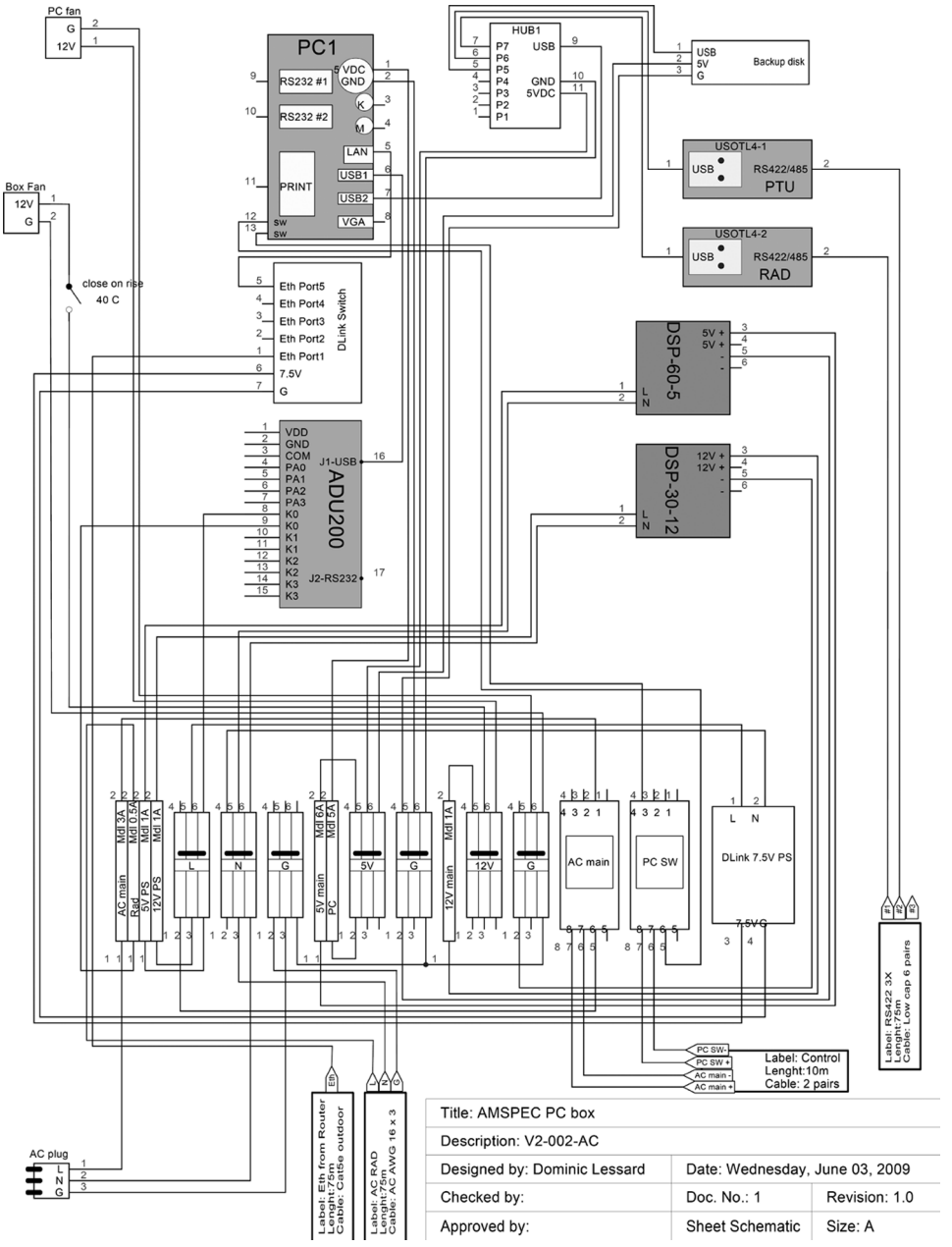

APPENDIX 2 Wiring diagrams computer module.